Xinnian Wang[1]
Department of Mechanical and Industrial Engineering, University of Illinois at Chicago, Chicago, IL 60607
e-mail: xwang313@uic.edu

Jevon Plog[1]
Department of Mechanical and Industrial Engineering, University of Illinois at Chicago, Chicago, IL 60607
e-mail: jplog2@uic.edu

Ketki M. Lichade
Department of Mechanical and Industrial Engineering, University of Illinois at Chicago, Chicago, IL 60607
e-mail: klicha2@uic.edu

Alexander L. Yarin[2]
Department of Mechanical and Industrial Engineering, University of Illinois at Chicago, Chicago, IL 60607;
School of Mechanical Engineering, Korea University, Seoul 136-713, South Korea
e-mail: ayarin@uic.edu

Yayue Pan[2]
Department of Mechanical and Industrial Engineering, University of Illinois at Chicago, Chicago, IL 60607
e-mail: yayuepan@uic.edu

Three-Dimensional Printing of Highly Conducting PEDOT: PSS-Based Polymers

Poly(3,4-ethylenedioxythiophene):poly(styrenesulfonic acid) (PEDOT:PSS) is one of the most successful conducting polymers for electronic applications. Most commonly, the spin coating process is used to fabricate PEDOT:PSS thin films from an aqueous solution, yet it is unsuitable for fabricating complicated two-dimensional (2D) structures. Extrusion-based additive manufacturing (AM) processes have been investigated for 3D printing PEDOT:PSS-based polymers with free-form architecture. However, such methods imply strict requirements on the rheological properties of materials and, as a result, have limited choices of appropriate materials. In the past, additives have been added to improve the 3D printing processability of PEDOT:PSS materials, which, however, usually deteriorate the electrical conductivity. This article reports a new type of PEDOT: PSS material capable of addressing the previously listed challenges and characterized by high processability and electrical conductivity (72 S/cm). In addition, a novel extrusion-based AM technology, electrostatically-assisted direct ink writing (eDIW), is investigated for printing materials containing PEDOT:PSS. The eDIW method prints lines at micro-scale resolution at an ultra-high speed (1.72 m/s). This combination is often deemed impossible in the framework of classical extrusion-based AM techniques. This work lays the foundation for future explorations of applications of PEDOT:PSS-based conducting polymers in fields that require superb properties and custom geometry, which were conventionally impossible. [DOI: 10.1115/1.4055850]

Keywords: PEDOT:PSS, conducting polymers, conductivity, 3D printing processability, direct ink writing, additive manufacturing

1 Introduction

Conducting polymers are considered a new generation of materials that exhibit the "electrical and optical properties of metals or semiconductors and which retain the attractive mechanical properties and processing advantages of polymers" [1]. Among different conducting polymers, poly(3,4-ethylenedioxythiophene):poly(styrene sulfonate) (PEDOT:PSS) is the most successful one in the industry [2]. PEDOT:PSS presents good water dispersibility, high stability, good film-forming properties, good conductivity, and satisfactory stretchability [3]. PEDOT:PSS is nowadays commercially produced on a large scale and sold for fundamental research and practical applications in academics and industry. Among different areas of its applications, PEDOT:PSS holds great promise in the field of organic electronics as transparent conductive oxides, hole conducting layer or electrochromic layer in a variety of devices from organic light-emitting diodes, organic photovoltaic devices, or electrochromics [4–6]. In the last few years, PEDOT:PSS has also been widely applied in electronic devices in different applications such as electrodes for electrophysiology, a variety of biosensors, organic electrochemical transistors, organic electronic ion-pump, electronic textiles, or electronic skin [7–9].

Commercially available PEDOT:PSS aqueous solutions are low-viscosity liquids with a zero-shear viscosity less than 1 Pa s sold for casting, dip coating, spin coating, lithography, and inkjet printing [10–12]. For instance, Srichan et al. used inkjet printing to fabricate PEDOT:PSS microstructure [10]. Dong et al. used spin coating to manufacture the PEDOT:PSS anode for semi-transparent inverted polymer solar cells [11]. Greco et al. fabricated an ultra-thin conductive PEDOT:PSS film by spin coating [12]. Although these manufacturing processes have made remarkable achievements in producing the PEDOT:PSS films, it is challenging or even impossible to fabricate complicated patterns, such as highly porous or self-standing structures, using these techniques.

In contrast to the aforementioned technologies, additive manufacturing (AM) techniques have been investigated for fabricating complex 2D structures using PEDOT:PSS-based conducting polymers and composites. To make it processable using AM techniques, the PEDOT:PSS aqueous solution usually needs to be modified by adding some additional chemicals or preprocessed using special techniques. For example, Heo et al. used stereolithography (SLA) to successfully fabricate conductive scaffolds by adding different concentrations of PEDOT:PSS nanofibers to the polyethylene glycol diacrylate solution [13]. Tao et al. fabricated multiwalled carbon nanotubes-polyethylene glycol microstructures using the two-photon polymerization process. The printed microstructures were further immersed into the PEDOT:PSS aqueous solution for PEDOT:PSS self-assembly on their surface [14]. Scordo et al. precipitated PEDOT using H_2SO_4 added to PEDOT:PSS solution. The PEDOT was then suspended in photosensitive resin for use in the SLA process [15]. Li et al. isolated solid PEDOT:PSS-polyethylene oxide (PEO) from solutions to produce filament for fused filament fabrication (FDM) [16].

[1]Euqally contributed to this article.
[2]Corresponding authors.
Manuscript received July 1, 2022; final manuscript received September 23, 2022; published online November 7, 2022. Assoc. Editor: Chinedum Okwudire.

Direct ink writing (DIW) is a versatile additive manufacturing process that controls the air pressure to dispense functional liquids (i.e., inks) onto a substrate along predefined paths to make an object. An ideal DIW ink should possess two rheological properties: shear-thinning and viscoelastic behavior. These properties ease flow through the nozzle while allowing shape retention after the extrusion [17]. However, as to our knowledge, very few studies have focused on the PEDOT:PSS rheological characteristics for the DIW process. Yuk et al. found that concentrations of PEDOT:PSS nanofibers within 1–4 wt% had low yield stress, which caused the extruded ink to spread on the substrate before solidification. However, a high concentration of PEDOT:PSS nanofibers (>8 wt%) would block the nozzle [18]. The PEDOT:PSS aqueous solution concentration is less than 4 wt% currently on the market [17], which does not have the appropriate viscoelastic property and thus not ideal for the DIW process. Increasing the concentration of the PEDOT:PSS ink takes multiple complex steps [18]. The first step is to isolate nanofibers from the purchased low-concentration PEDOT:PSS aqueous solution and then re-disperse the specific concentration of nanofibers in the deionized water with various mixing methods to make a homogeneous high-concentration PEDOT:PSS aqueous solution [18]. Liu et al. demonstrated that the hydrophilic 2D material (Ti3C2 MXene) could significantly improve the PEDOT:PSS aqueous solution's rheological properties [19].

In addition, the pristine commercial PEDOT:PSS has limited conductivity (~1 S/cm), which is too low to be used for fabricating some electronic devices [17]. In the last few decades, scientists found that adding polar organic solvents such as dimethyl sulfoxide (DMSO), ethylene glycol, and glycerol to the PEDOT:PSS aqueous solution could significantly improve the conductivity by many orders of magnitude [20]. For example, Hokazono et al. found that the conductivity could be increased up to 600 S/cm by adding 5% DMSO [21]. Also, Lee et al. reported that glycerol could improve the conductivity to 450 S/cm [22]. Despite these liquid-phase compounds having succeeded in enhancing the PEDOT:PSS conductivity, limitations are apparent because of their high boiling temperature characteristic. Those high conductive inks cannot be solidified at room temperature or a temperature < 60 °C, which poses challenges or additional requirements to the manufacturing process and equipment. Finding an appropriate polymer that can enhance the conductivity and simultaneously increase the processability (i.e., the ability to be extruded and solidified after the extrusion without requiring high temperatures) is essential.

Against the background, to improve the PEDOT:PSS conductivity and printability in DIW, we develop a new type of PEDOT:PSS-based ink. Two polymers, poly(*N*-isopropylacrylamide) (PNIPAM) and polyethylene oxide (PEO), are investigated in blends using the PEDOT:PSS solutions. PEO is a biocompatible material commonly used to enhance the viscosity of materials for extrusion-based 3D printing [23]. PEO gels possess shear-thinning behavior at any concentration [24]. PNIPAM is an eco-friendly temperature-responsive polymer, also commonly used as a thickener to increase the viscosity of a solution [25]. In addition, we also develop a novel extrusion-based additive manufacturing technology, electrostatically-assisted direct ink writing (eDIW), for printing PEDOT:PSS materials at an ultra-high-speed and simultaneously at micro-scale resolution. The rest of this article is organized as follows. Section 2 discusses the development of PEDOT:PSS-based inks for DIW, including an approach to prepare the PEDOT:PSS-based ink and characterizations of the rheological and conductive properties of those solutions. Section 3 presents the eDIW process for printing PEDOT:PSS polymers. Section 4 discusses some PEDOT:PSS patterns fabricated by the eDIW and DIW. The work is summarized in Sec. 5.

2 Development of Highly Conducting and Printable Polymers

2.1 Preparation of PEDOT:PSS-Based Ink. A dark blue PEDOT:PSS (CLEVIOS™ PH 1000) purchased from Heraeus (Hanau, Germany) was used as the base conducting polymer. PNIPAM and PEO powders from Sigma-Aldrich (Burlington, MA) were investigated for tuning the ink rheological properties to increase its printability. All these materials were used as received.

To prepare PEDOT:PSS/PNIPAM and PEDOT:PSS/PEO inks, 1 L of pure PEDOT:PSS solution was first stirred for 3 h to remove aggregates. Then, we equally divided the PEDOT:PSS solution into two different groups. PEO powders were added in the first group of PEDOT:PSS solution with the ratio of 20 wt%, 36 wt%, 52 wt%, 75.8 wt%, 80 wt%, and 90.2 wt% (based on the total solid weight of PEO and PEDOT:PSS). PNIPAM powder was added to the second group of PEDOT:PSS solutions with a ratio of 20 wt%, 36 wt%, and 52 wt% (based on the total solid weight of PNIPAM and PEDOT:PSS). To make homogeneous and stable PEDOT:PPS/PEO and PEDOT:PSS/PNIPAM solutions, we used a magnet stirrer to stir these blends for 17 h at room temperature. The materials' chemical modules and the preparation processes are shown in Fig. 1.

2.2 Characterization of Rheological Properties for Extrusion-Based Additive Manufacturing. Rheological properties of the prepared PEDOT:PSS-based polymer inks were characterized by a rotational rheometer (Kinexus Ultra+, NETZSCH Instruments, Burlington, MA) with a constant temperature (25 °C). The gap distance between the two parallel plates was set at 0.2 mm during the measurement, and the range of the shear rate was from 1 s^{-1} to 100 s^{-1}. The acquired data are shown in Fig. 2(*a*). As expected, all samples (PEDOT:PSS/PEO and PEDOT:PSS/PNIPAM polymers) have shear-thinning behavior. With an increase in shear rate, these materials' viscosities decrease, allowing ink to flow easier through the nozzle. Meanwhile, both PEO and PNIPAM can increase the PEDOT:PSS solution viscosity (Fig. 2(*b*)) at a low shear rate (1 s^{-1}), which will help to keep filament shape stable after being dispensed on the substrate. Besides, PNIPAM has a more significant impact on increasing the PEDOT:PSS solution viscosity.

2.3 Characterization of Conductivity. The PEDOT:PSS contains two ionomers. One is the positively charged PEDOT and the other one is the negatively charged PSS. The Coulombic interactions between the short PEDOT chain and long PSS chain make the PEDOT:PSS nanofiber stable in the aqueous solution [26]. In addition, PEDOT has two structures, benzoid structure and quinoid structure (Figs. 3(*a*) and 3(*b*)). The quinoid structure exhibits higher conductivity because it has delocalized ions. However, a commercial PEDOT:PSS aqueous solution contains both PEDOT structures. Furthermore, the nonionic dopant PSS causes the low conductivity of the PEDOT:PSS solution [27].

It is commonly believed that PEO and PNIPAM would improve PEDOT:PSS conductivity in the same way by weakening the Coulombic interactions between the PEDOT and PSS chains [28,29]. It gives the chance to change the resonant structure of PEDOT chains from the benzoid structure to the quinoid structure [30]. Meanwhile, PEO could also connect PSS chains (Fig. 3(*c*)) so that the PEDOT chains can be linearly reoriented [31,32].

To validate and compare the conductivity of the PEDOT:PSS/PEO and PEDOT:PSS/PNIPAM polymers printed by the extrusion-based AM process, we printed films using a DIW printer and the inks prepared as explained in Sec. 2.1. Before measuring the resistance, the printed films were dried at 60 °C for 30 min to evaporate water inside the structure.

All the printed samples were characterized and compared via four-point probe testing. Equally spaced probes with a point-of-contact radius measuring 1 mm were repeatedly pressed onto 20-by-20 mm thin films. The current was supplied to the outer probes from a Keithley 2400 sourcemeter, while the voltage was measured by a Fluke 8845 precision multimeter. Each conductive ink was printed into six samples. We tested each sample twice at the same location of the film. The error bar shown in Fig. 4 is one

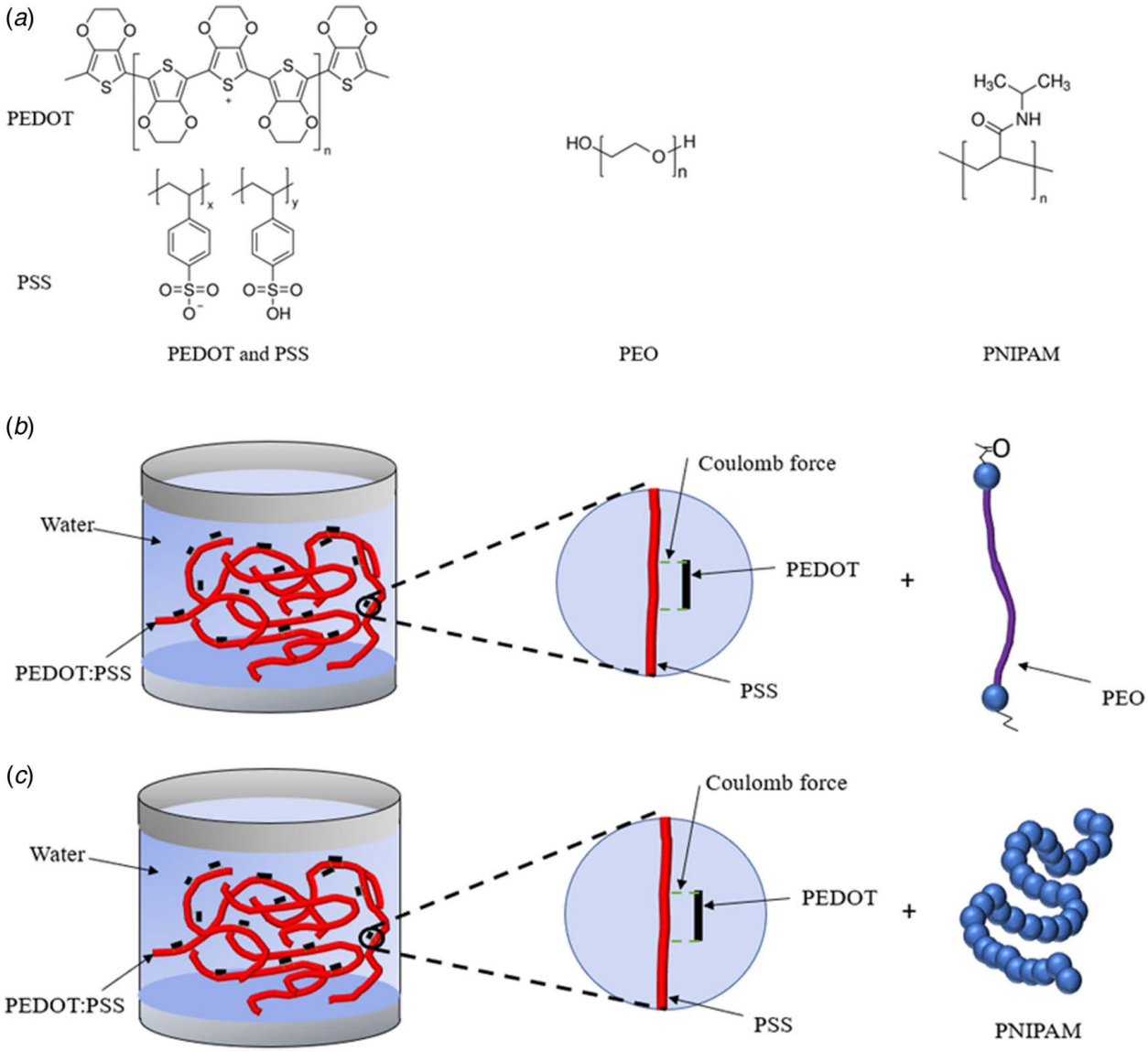

Fig. 1 PEDOT:PSS/PEO and PEDOT:PSS/PNIPAM preparation: (*a*) chemical structure of PEDOT, PSS, PEO, and PNIPAM, (*b*) PEDOT:PSS/PEO preparation process, and (c) PEDOT:PSS/PNIPAM preparation process

standard deviation, while the resulting sheet resistances are plotted in Fig. 4(*a*). After measuring the sample thicknesses with a surface profiler, the sheet resistances were converted to bulk conductivity by using the following equation and plotted in Fig. 4(*b*)

$$\text{Electrical conductivity} = \frac{1}{\text{Sheet resistance} \times \text{Layer thickness}}$$

It can be seen that the polymer conductivity increases with the increase of the PEO weight ratio in the ink and reaches a peak point around 52 wt%. Then, the conductivity decreases with the increase in the PEO weight ratio. The highest conductivity is observed from the samples printed using PEDOT:PSS/ 52 wt% PEO solution. It should be noted that with the exception of 20 wt % PEO, which caused no change, the remaining PEO solutions all had a positive effect on conductivity. In our opinion, a low weight ratio of PEO was unlikely to weaken the Coulomb interaction between PEDOT chains and PSS chains, nor could it cause the chains to be reoriented. In addition, since PEO itself has negligible electrical conductivity, it will decrease the electrical conductivity of the liquid material if there are many free PEO macromolecules present. While the measurement results revealed that the addition of PNIPAM decreased the conductivity, it should be emphasized that the additional polymers did increase the processability of PEDOT:PSS, which increase the PEDOT:PSS viscoelasticity. The semiconductors often span a vast range of conductivities. The conductivity tunability offered by PNIPAM (while producing successful prints) might still prove beneficial, even though the value is lower than pristine PEDOT:PSS. In theory, a high ratio of insulating polymers will decrease PEDOT:PSS conductivity [28]; a possible explanation is that 20 wt% is a high ratio for PNIPAM in the PEDOT:PSS/PNIPAM ink, and a lower weight ratio of PNIPAM (<20 wt%) may lead to a positive effect on the conductivity. In future, we plan to revisit this question.

3 eDIW Process for Printing PEDOT:PSS-Based Polymers

DIW is a widely used extrusion-based additive manufacturing process that controls the pressure inside the extruder to dispense functional liquid or paste ink on a substrate along predefined paths to build a three-dimensional (3D) model. The ideal DIW

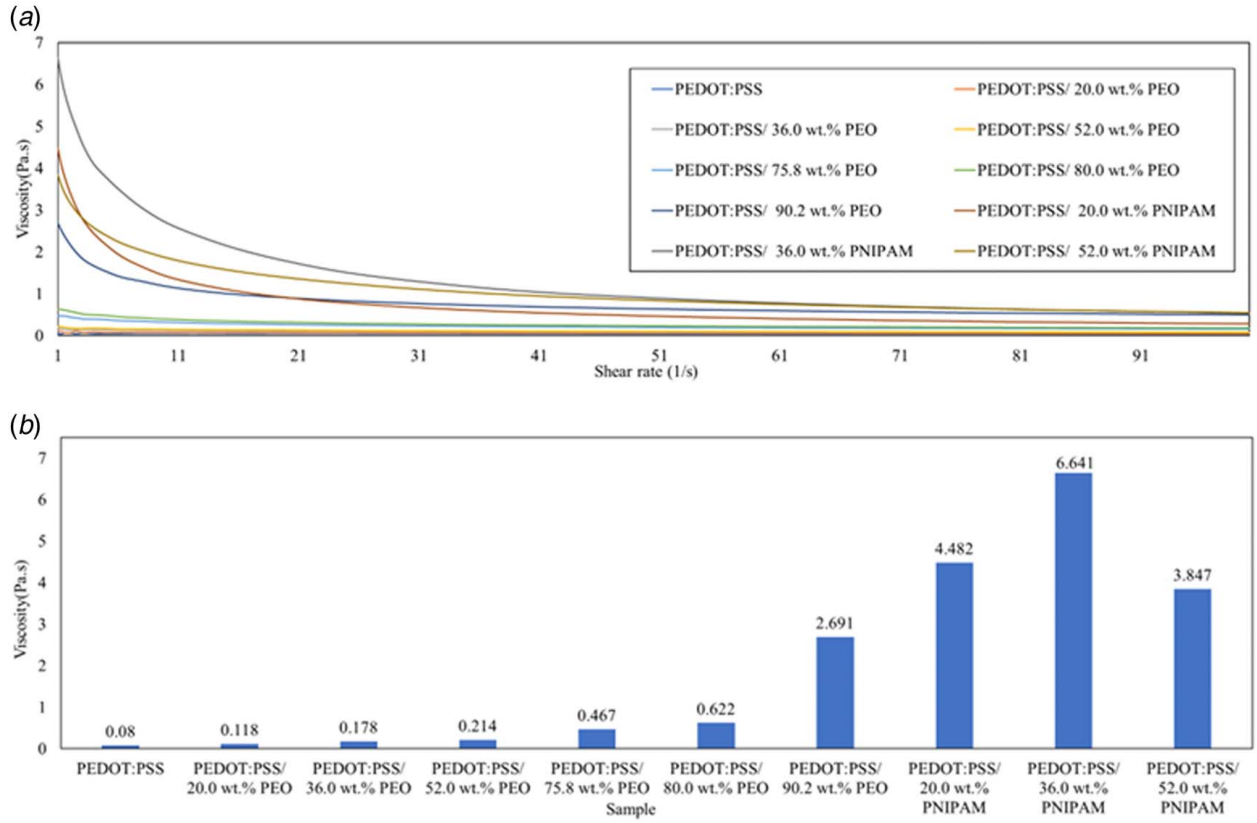

Fig. 2 PEDOT:PSS/PEO and PEDOT:PSS/PNIPAM rheological properties: (*a*) PEDOT:PSS/PEO and PEDOT:PSS/PNIPAM flow curves in simple shear and (*b*) viscosity of PEDOT:PSS/PEO and PEDOT:PSS/PNIPAM at a low shear rate (1 s^{-1})

ink should possess two rheological properties, a shear-thinning behavior and a viscoelastic behavior, to allow it to be extruded from a nozzle and retain its shape after the extrusion [33]. According to the rheological properties characterized in Sec. 2.2, the PEDOT:PSS/ 52 wt% PEO ink is supposed to be printable in DIW when the process parameter settings, including speed and pressure, are appropriate. In addition, in our previous study [34], it was found that by integrating an electric field (EF), for the same ink, a higher speed, a more stable printing, and a higher resolution could be achieved simultaneously. We call this process an electric field-assisted direct ink writing (eDIW).

To explore the effectiveness of eDIW on printing the developed PEDOT:PSS/ 52 wt% PEO ink, we tested the ink in both DIW and eDIW setup. The eDIW setup is developed by simply integrating an external electric field with the extrusion system and using a belt substrate for the high translational speed. The DIW setup is shown in Fig. 5(*a*). It consists of a syringe filled with liquid ink, a pressure generator, and an air regulator for controlling the vacuum and the air pressure in syringe barrel for ink dispensing, a camera for monitoring the ink-writing process in situ, and a platform that could move along *X*-axis and be heated from the room temperature up to 125 °C, a Z linear stage, and a Y stage that could move the printing needle along the *Z*- and *Y*-axes. This hardware system has a limited *X*-axis moving speed and the *Y*-axis moving speed of 0.5 m/s. For high-speed printing on the belt system, velocities are measured using a high-speed camera and scale. All printings were started after the translational speed achieved steady state and were ended before the deceleration.

The schematic diagram of the eDIW setup and the eDIW prototype machine developed in this study are shown in Figs. 5(*b*) and 5(*c*), respectively. In eDIW, the air pressure in the printing needle is controlled by a pressure generator and the printing needle can move along the *Z*-direction. The belt can move along the *Y*-axis with the speed up to 13.2 m/s. The printing needle is grounded

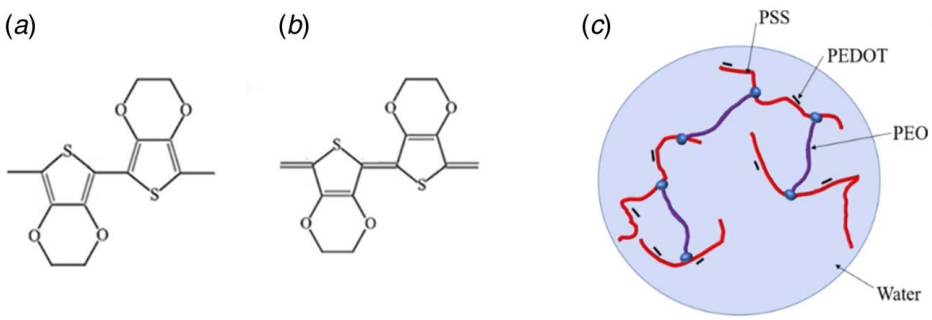

Fig. 3 Chemical structure of PEDOT: (*a*) benzoid structure, (*b*) quinoid structure, and (*c*) PEDOT:PSS/PEO

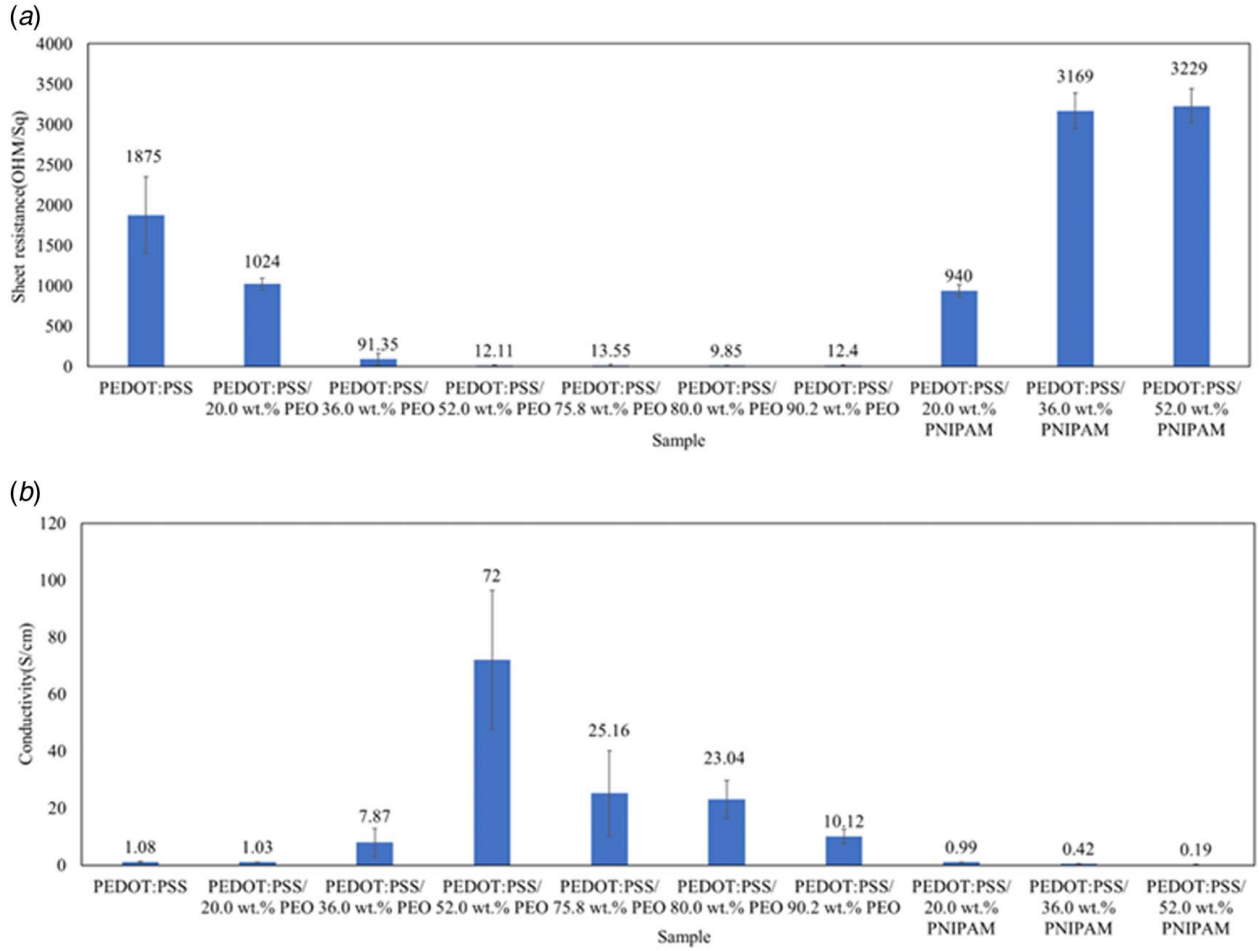

Fig. 4 Results of the electrical testing of different polymer weight ratios added to pristine PEDOT:PSS: (*a*) sheet resistance and (*b*) electrical conductivity

and an additional governing electrode is placed by the extruder tip orifice. The grounded printing needle is directly connected to the high-voltage power supply, which concurrently supplies the positive charge to the governing electrode. Voltages applied to the governing electrode were in the 2–4 kV range, with the EF strength being limited to ~3 kV/mm by the dielectric breakdown.

The governing electrode is placed just in front of the extruder (relative to the motion) and always pulls the ink in the direction opposite to that of the substrate relative motion. To generate a driving pressure for ink extrusion, a commercial pressure controller (Nordson Ultimus I) supplemented with 22-gauge stainless steel printing needles was used for experiments. We chose a larger needle size for high-speed experiments, which helped increase the ink extrusion volumetric flowrate. Unlike the DIW processes in which a larger needle commonly results in a lower resolution, the larger needle in the eDIW process revealed similar printing characteristics (e.g., resolution, accuracy) to the printing results of smaller needle diameters, thanks to the effect of the electric field. The pressure controller allowed for a well-defined pressure pulse (1–80 psi) to be applied to the ink within the needle for the programmed time duration. The governing electrode was bent from a 0.5 mm copper wire with care being taken while positioning not to let the wire extend below the edge of the printing needle.

Before starting an electrically modified print, several considerations should be taken to plan the eDIW process to print samples with the desired quality. First, general knowledge of how the chosen ink behaves during printing without the electric field helps us to identify a rough range of proper process settings, including voltage, standoff distance, pressure, and speed. Higher pressure is applied to extrude the prepared PEDOT:PSS-based inks with a higher weight ratio of added powders. As substrate translational speed increases, a higher voltage is necessary than for prints with lower velocities. This relationship makes sense as a larger force is needed to keep the proceeding triple line from being pulled back by the substrate. Higher translational speeds require prolonged accelerations. It should be emphasized that the EF helps to minimize these effects, which are generally seen as gradual widening/thinning of the line. However, as long as EF strength stays below the dielectric breakdown limit of 3 kV/mm, no harmful effect has been noted in the eDIW process.

4 Electric Field-Assisted Direct Ink Writing of PEDOT:PSS-Based Polymers

4.1 Printability in eDIW Process. To test the printability of the highly conductive PEDOT:PSS/52 wt% PEO ink developed in this study, we first fabricated a few samples with a conventional DIW process without an electric field. We found that the ink can be successfully printed by DIW with a pressure of 10 psi, and a substrate translational speed not higher than a threshold speed of 0.15 m/s. The threshold speed was determined by repeatedly printing lines at the increasing speed until failure. When the substrate moving speed exceeds this threshold, the DIW printing becomes unstable, and defects such as discontinuity occur. Figure 6(*a*) shows the side view of the DIW process with a substrate translational velocity of 0.257 m/s, which is above the critical threshold speed. It is important to note that the critical threshold velocity will change based on needle diameter, length, and driving

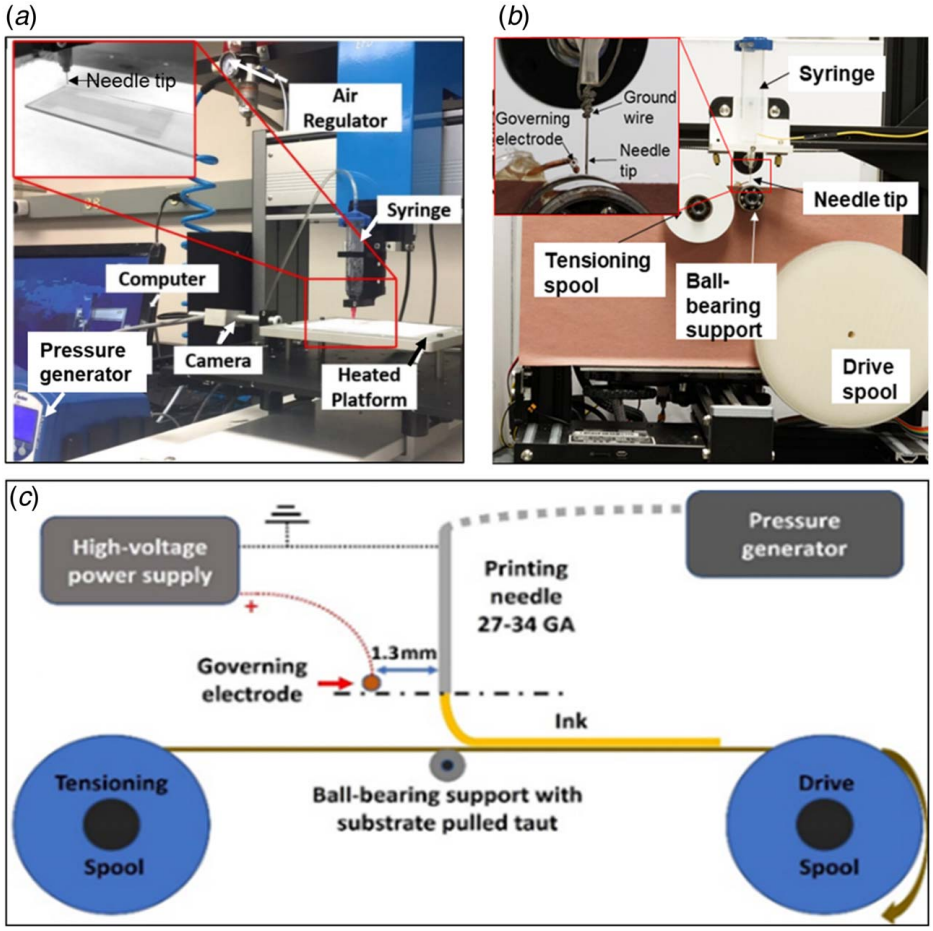

Fig. 5 (*a*) A DIW prototype used for printing the developed polymers in this study: maximum substrate moving speed is limited by the hardware, which is 0.5 m/s, (*b*) an eDIW prototype, and (*c*) the schematic of the eDIW prototype

pressure, so all were constant between the tests. Figures 6(*b*) and 6(*c*) show the top views of the printed ink line after solidification. It can be seen that the line printing failed with periodic discontinuities, indicating failure after the critical speed threshold was surpassed.

To address this challenge, the EF was applied to create the eDIW configuration, as explained in Section 3. Figure 7(*a*) shows the same side view as shown in Fig. 6(*a*), while the substrate translational velocity in Fig. 7(*a*) has been increased to 1.72 m/s, i.e., about 650% of the highest possible velocity for successful printing

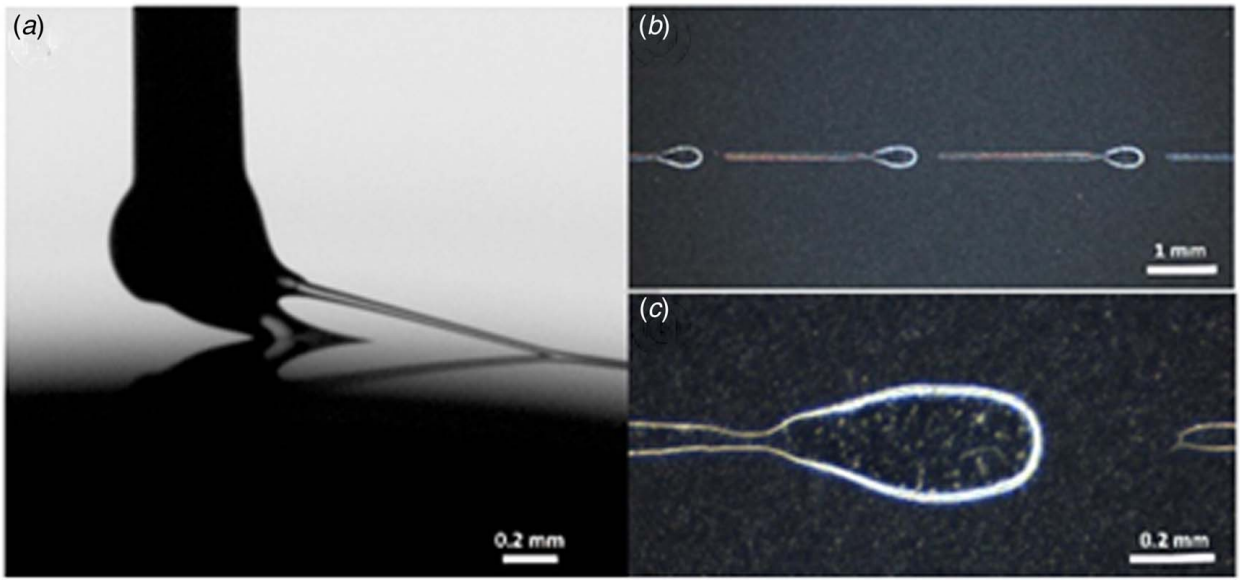

Fig. 6 PEDOT:PSS/52 wt% PEO solution extruded on substrate moving at a translational speed of 0.257 m/s: (*a*) side view with no EF applied, (*b*) top view of dried ink at 32× magnification, and (*c*) top view of dried ink at 193× magnification

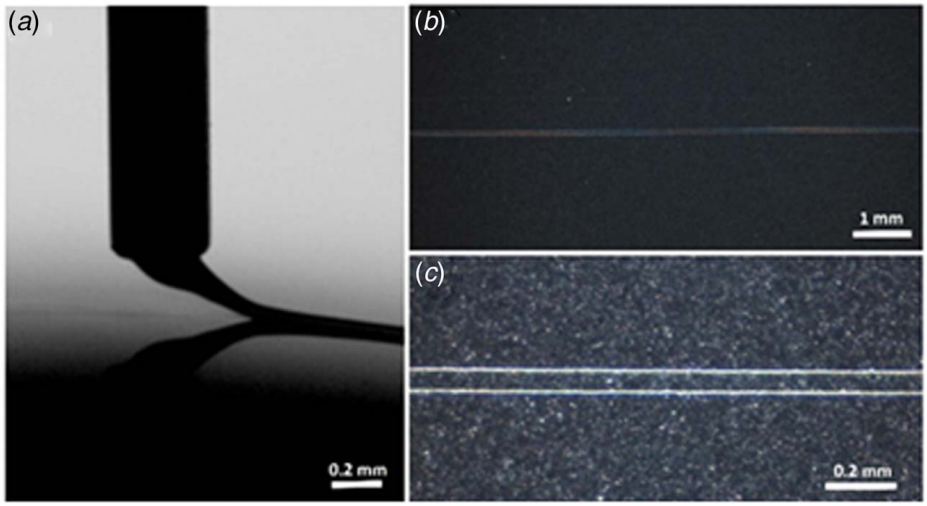

Fig. 7 PEDOT:PSS/ 52 wt% PEO solution printed on a substrate moving at a translational speed of 1.72 m/s and with 2.5 kV applied to the governing electrode: (*a*) side view of the ink filament extruded from the needle orifice and dispensed on the belt substrate, (*b*) top view of the dried ink line at 32× magnification, and (c) top view of dried ink line at 193× magnification

without the EF applied. With the electric field applied, intact continuous lines were successfully printed at the same speeds as without EF and even at a much higher speed of 1.72 m/s. These beneficial enhancements result from the Coulomb force between the electrode and extruded ink pulling in the direction of printing and allowing faster translational speed, thinner trace widths, and improved deposition. Figures 7(*b*) and 7(*c*) are taken from a top view at two different magnifications. The ink line width is 64 μm. It is worthwhile to highlight how straight and accurate dried PEDOT:PSS-based polymer traces in Fig. 7 are with no signs of discontinuities or bulging.

To make direct comparisons, the DIW process without the EF was slowed down to 0.15 m/s to allow for printing continuous lines, as shown in Figs. 8(*a*)–8(*c*). While not extremely noticeable, a slight meandering is shown in Figs. 8(*a*)–8(*c*). Figure 8(*c*) is the same print line shown in Fig. 8(*a*), which was just zoomed out to show more length. Besides the meandering previously mentioned, undesirable bulging can also be observed along the trace line in Fig. 8(*c*).

In contrast, the printed line in Fig. 8(*b*) is much more accurate and straight. No meandering or bulging defects were observed in the line shown in Fig. 8(*b*). The continuous straight line in Fig. 8(*b*) was printed by eDIW with 2.5 kV applied to the governing electrode and a substrate translational velocity of 1.72 m/s. Figure 8(*b*) also highlights the increased resolution when compared to the line printed by DIW in which no EF was applied as shown in Fig. 8(*a*). The width of the line printed by DIW as shown in Figs. 8(*a*)–8(*c*) is 245 μm, while the width of the line printed by eDIW as shown in Fig. 8(*b*) is 64 μm.

4.2 Test Cases of PEDOT:PSS-Based Polymer Parts. To validate the printability of the highly electrically conductive PEDOT:PSS/PEO ink in DIW and eDIW, test cases were performed in both DIW and eDIW. First, to validate the electric performance of the printed PEDOT:PSS/52 wt% PEO pattern, we fabricated a thin PET film (10 mm by 50 mm by 0.04 mm) on a Kapton tape using the DIW process without electric field applied. The sample was printed with a pressure of 0.4 psi, a speed of 30 mm/s, a standoff distance of 0.104 mm, and a 23-gauge (0.6 mm) needle.

An LED circuit was constructed to test the conductivity of the sample, as shown in Fig. 9. The anode of LED was touching the right side of the PEDOT:PSS/52 wt% PEO film. The cathode of LED and the left-hand side of the film were connected to a power

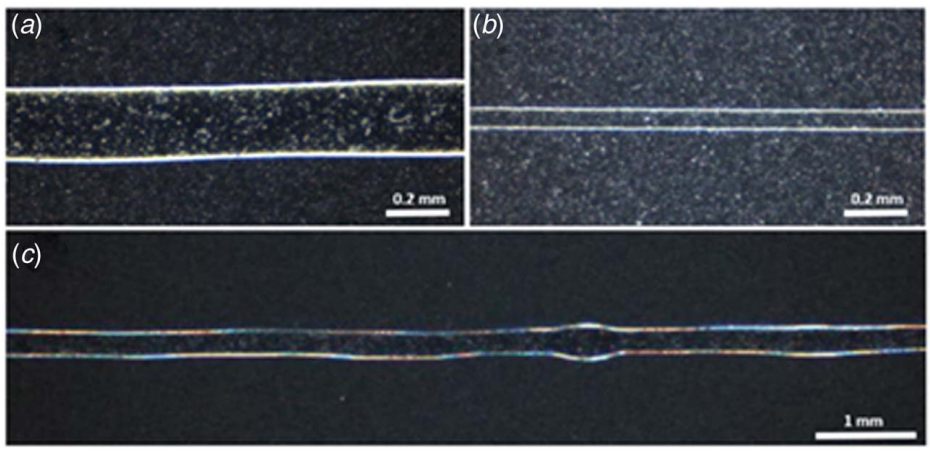

Fig. 8 PEDOT:PSS/52 wt% PEO solution extruded on a substrate moving at various translational velocities: (*a*) top view of dried ink with no EF applied and printed with translational velocity of 0.15 m/s, (*b*) top view of dried ink with 2.5 kV applied to the electrode and a translational velocity of 1.72 m/s, and (c) expanded top view of dried ink with no EF during printing

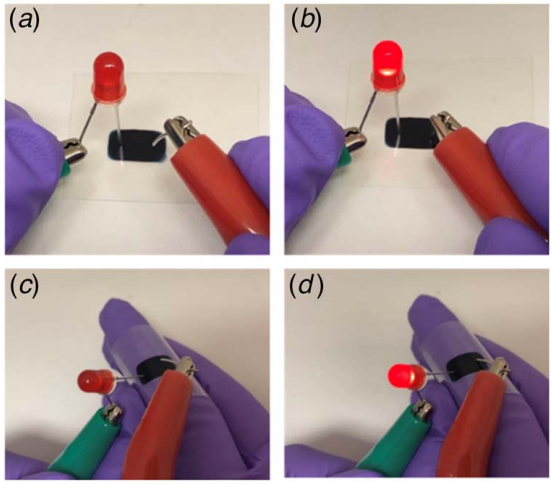

Fig. 9 (*a*) LED light is OFF when the power supply is off and when PEDOT:PSS/52 wt% PEO film was put on a flat surface, (*b*) LED light in ON when the PEDOT:PSS/52 wt% PEO film was put on a flat surface and connected to the power supply with 2.8 V, (c) LED light is OFF when no power is provided, and the PEDOT:PSS/52 wt% PEO film was bent, and (*d*) LED light is ON when the PEDOT:PSS/52 wt% PEO film was bent by wrapping around the index finger and was connected to the power supply of 2.8 V.

supply that provided 2.8 V. Figures 9(*a*) and 9(*b*) show that LED light in the OFF state when the voltage is 0 and in the ON state when a voltage of 2.8 V is provided and the PEDOT:PSS/52 wt% PEO film was put on a flat substrate. The real-time video of the experiment (video1) can be found in the Supplementary Materials on the ASME Digital Collection.

To test the flexibility of the printed film and its electrical performance in a bended state, the film was bent along its long axis by wrapping it around an index finger, and the same LED circuit was tested. When the power supply is off, the LED light is off, as shown in Fig. 9(*c*). When the power supply is turned on, the LED light is on as shown in Fig. 9(*d*). The real-time video of the experiment (video2) can be found in the Supplementary Materials.

To test the printability of PEDOT:PSS/PEO ink in DIW, we fabricated a cross diamond pattern with three layers on a glass substrate and a circular grid pattern with five layers on a Kapton tape substrate. The printed samples are shown in Fig. 10. A manual adjustment of the air pressure and printing speed was required to ensure the printed line was straight, continuous, and of the expected width. A 0.9 psi pressure and 23-gauge needle were used to print these patterns. The printing speed was set to be 30 mm/s. A standoff distance of 0.104 mm was used. As shown in Fig. 10, both structures have been printed successfully with no breakpoint or bulge. As shown in Fig. 10, the dark color was uniform, implying the PEDOT:PSS and PEO were evenly distributed in the dispensed ink before and after drying.

To test the printability of the developed PEDOT:PSS/52 wt% PEO ink in eDIW, we printed a wave pattern (three layers) and

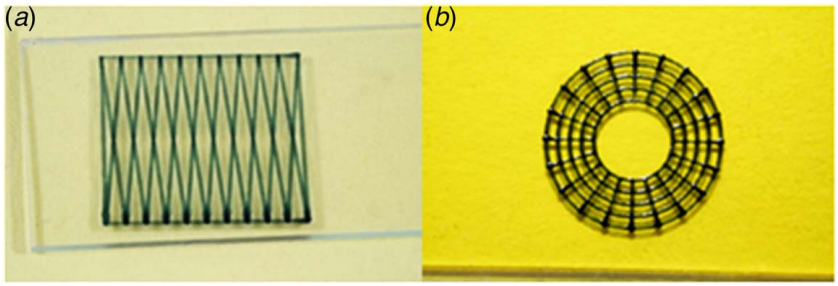

Fig. 10 Structures printed by the DIW process: (*a*) a printed cross diamond structure and (*b*) a printed circular grid structure

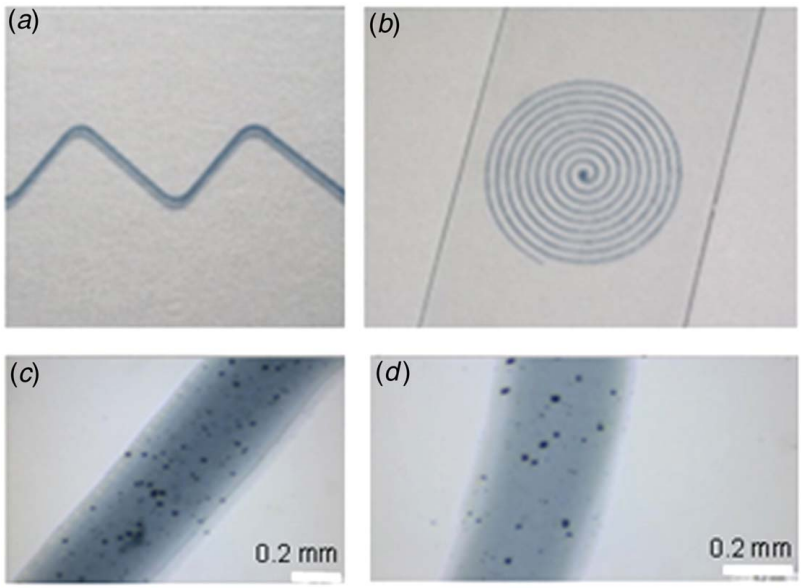

Fig. 11 Patterns printed by eDIW process: (*a*) optical picture of the wave pattern, (*b*) optical picture of the circular pattern, (c) microscopic image of the wave pattern, and (*d*) microscopic image of the circular pattern

a circular pattern (2 layers) on the glass substrate by eDIW with 3 kV applied to the electrode. A 25-gauge needle (0.5 mm needle tip diameter) was used to fabricate the pattern, and the substrate translational speed was 50 mm/s. The pressure was set to be 0.8 psi. Figures 11(*a*) and 11(*b*) show the optical images of the printed patterns. Microscopic images with 193× magnification of the printed patterns are shown in Figs. 11(*c*) and 11(*d*), respectively. The line widths were measured on the microscopic images. The line widths of the wave pattern and the circular pattern are 0.486 mm and 0.479 mm, respectively. The black dots on the microscopic images are PEDOT:PSS nanofibers, which are almost uniform. The previous study utilized an eDIW to fabricate a straight line at an ultra-high speed (i.e., several meters per second), which is orders of magnitude faster than the common speeds of DIW processes (i.e., several millimeters per second). It is the first time that eDIW has been used for a complex structure. The results of the experiment indicate that eDIW has no adverse effect on the printed results. The printing speed of complex objects will be increased in the future work.

5 Conclusion

This study develops a new type of 3D printable and highly conducting PEDOT:PSS-based polymer ink and a novel eDIW process for printing this type of inks at a significantly higher speed (meters per second) that is impossible with the conventional DIW process. The 3D printable conducting inks developed in this study are composed of two compounds: (i) PEDOT:PSS as the base conducting polymer and (ii) PEO or PNIPAM as the second dopant, which is used to improve the rheological properties for enhanced printability and conductivity. The pristine commercial PEDOT:PSS is a low-viscosity and nonviscoelastic liquid. The dispensed liquid cannot retain its shape before solidification. PEO and PNIPAM work as thickeners that can effectively increase the viscosity of the PEDOT:PSS aqueous solution, making it printable in the extrusion-based additive manufacturing processes. In addition, the PEO doping is shown to be effective for enhancing the PEDOT:PSS conductivity. The PEDOT:PSS/52 wt% PEO solution exhibits the highest conductivity (72 S/cm), which is almost 70 times of the pristine PEDOT:PSS conductivity (1.08 S/cm). In addition, a novel extrusion-based additive manufacturing process, eDIW, was tested for printing the highly conducting PEDOT:PSS/52 wt% PEO material. By applying an external electric field, eDIW can print the developed PEDOT:PSS-based polymer ink at an ultra-high speed (1.72 m/s) and micro-scale resolution. Such high-speed and high-resolution extrusion-based 3D printing capability will open a new venue for a high-throughput production of electronic components, especially those that require meter-scale large conductive pattern size along with micro-scale resolutions. Future work will focus on further exploring the properties of the printed PEDOT:PSS-based polymers and the effects of the process parameters on the printed properties.

Funding Data

- National Science Foundation (NSF) Grant No 1825626.

Conflict of Interest

There are no conflicts of interest.

Data Availability Statement

The authors attest that all data for this study are included in the paper.

References

[1] Heeger, A. J., 2001, "Nobel Lecture: Semiconducting and Metallic Polymers: The Fourth Generation of Polymeric Materials," Rev. Mod. Phys., **73**(3), pp. 681–700.

[2] Groenendaal, L., Jonas, F., Freitag, D., Pielartzik, H., and Reynolds, J. R., 2000, "Poly(3,4-Ethylenedioxythiophene) and Its Derivatives: Past, Present, and Future," Adv. Mater., **12**(7), pp. 481–494.

[3] Dominguez-Alfaro, A., Gabirondo, E., Alegret, N., De León-Almazán, C. M., Hernandez, R., Vallejo-Illarramendi, A., Prato, M., and Mecerreyes, D., 2021, "3D Printable Conducting and Biocompatible PEDOT-Graft-PLA Copolymers by Direct Ink Writing," Macromol. Rapid Commun., **42**(12), p. e2100100.

[4] Liu, H., Li, Q., Zhang, S., Yin, R., Liu, X., He, Y., Dai, K., et al., 2018, "Electrically Conductive Polymer Composites for Smart Flexible Strain Sensors: A Critical Review," J. Mater. Chem. C Mater. Opt. Electron. Devices, **6**(45), pp. 12121–12141.

[5] Hu, F., Xue, Y., Xu, J., and Lu, B., 2019, "PEDOT-Based Conducting Polymer Actuators," Front. Robot. AI, **6**, p. 114.

[6] Lee, I., Kim, G. W., Yang, M., and Kim, T.-S., 2016, "Simultaneously Enhancing the Cohesion and Electrical Conductivity of PEDOT:PSS Conductive Polymer Films Using DMSO Additives," ACS Appl. Mater. Interfaces, **8**(1), pp. 302–310.

[7] Zeng, R., Wang, W., Chen, M., Wan, Q., Wang, C., Knopp, D., and Tang, D., 2021, "CRISPR-Cas12a-Driven MXene-PEDOT:PSS Piezoresistive Wireless Biosensor," Nano Energy, **82**, p. 105711.

[8] Keene, S. T., van der Pol, T. P. A., Zakhidov, D., Weijtens, C. H. L., Janssen, R. A. J., Salleo, A., and van de Burgt, Y., 2020, "Enhancement-Mode PEDOT:PSS Organic Electrochemical Transistors Using Molecular DE-Doping," Adv. Mater., **32**(19), p. e2000270.

[9] Zhao, P., Zhang, R., Tong, Y., Zhao, X., Zhang, T., Tang, Q., and Liu, Y., 2020, "Strain-Discriminable Pressure/Proximity Sensing of Transparent Stretchable Electronic Skin Based on PEDOT:PSS/SWCNT Electrodes," ACS Appl. Mater. Interfaces, **12**(49), pp. 55083–55093.

[10] Srichan, C., Saikrajang, T., Lomas, T., Jomphoak, A., Maturos, T., Phokaratkul, D., Kerdcharoen, T., and Tuantranont, A., 2009, "Inkjet Printing PEDOT:PSS Using Desktop Inkjet Printer," 2009 6th International Conference on Electrical Engineering/Electronics, Computer, Telecommunications and Information Technology, Chonburi, Thailand, May 6–9.

[11] Dong, Q., Zhou, Y., Pei, J., Liu, Z., Li, Y., Yao, S., Zhang, J., and Tian, W., 2010, "All-Spin-Coating Vacuum-Free Processed Semi-Transparent Inverted Polymer Solar Cells With PEDOT:PSS Anode and PAH-D Interfacial Layer," Org. Electron., **11**(7), pp. 1327–1331.

[12] Greco, F., Zucca, A., Taccola, S., Menciassi, A., Fujie, T., Haniuda, H., Takeoka, S., Dario, P., and Mattoli, V., 2011, "Ultra-Thin Conductive Free-Standing PEDOT/PSS Nanofilms," Soft Matter, **7**(22), p. 10642.

[13] Heo, D. N., Lee, S.-J., Timsina, R., Qiu, X., Castro, N. J., and Zhang, L. G., 2019, "Development of 3D Printable Conductive Hydrogel With Crystallized PEDOT:PSS for Neural Tissue Engineering," Mater. Sci. Eng. C Mater. Biol. Appl., **99**, pp. 582–590.

[14] Tao, Y., Wei, C., Liu, J., Deng, C., Cai, S., and Xiong, W., 2019, "Nanostructured Electrically Conductive Hydrogels Obtained via Ultrafast Laser Processing and Self-Assembly," Nanoscale, **11**(18), pp. 9176–9184.

[15] Scordo, G., Bertana, V., Scaltrito, L., Ferrero, S., Cocuzza, M., Marasso, S. L., and Pirri, C. F., 2019, "A Novel Highly Electrically Conductive Composite Resin for Stereolithography," Mater. Today Commun., **19**, pp. 12–17.

[16] Li, H., Mao, P., Davis, M., and Yu, Z., 2021, "PEDOT: PSS-Polyethylene Oxide Composites for Stretchable and 3D-Printed Thermoelectric Devices," Compos. Commun., **23**, p. 100599.

[17] Shi, H., Liu, C., Jiang, Q., and Xu, J., 2015, "Effective Approaches to Improve the Electrical Conductivity of PEDOT:PSS: A Review," Adv. Electron. Mater., **1**(4), p. 1500017.

[18] Yuk, H., Lu, B., Lin, S., Qu, K., Xu, J., Luo, J., and Zhao, X., 2020, "3D Printing of Conducting Polymers," Nat. Commun., **11**(1), p. 1604.

[19] Liu, J., Mckeon, L., Garcia, J., Pinilla, S., Barwich, S., Möbius, M., and Nicolosi, V., 2022, "Additive Manufacturing of Ti3C2-MXene-Functionalized Conductive Polymer Hydrogels for Electromagnetic-Interference Shielding," Adv. Mater., **34**(5), p. 2106253.

[20] Kim, Y. H., Sachse, C., Machala, M. L., May, C., Müller-Meskamp, L., and Leo, K., 2011, "Highly Conductive PEDOT:PSS Electrode With Optimized Solvent and Thermal Post-Treatment for ITO-Free Organic Solar Cells," Adv. Funct. Mater., **21**(6), pp. 1076–1081.

[21] Hokazono, M., Anno, H., and Toshima, N., 2014, "Thermoelectric Properties and Thermal Stability of PEDOT:PSS Films on a Polyimide Substrate and Application in Flexible Energy Conversion Devices," J. Electron. Mater., **43**(6), pp. 2196–2201.

[22] Lee, M.-W., Lee, M.-Y., Choi, J.-C., Park, J.-S., and Song, C.-K., 2010, "Fine Patterning of Glycerol-Doped PEDOT:PSS on Hydrophobic PVP Dielectric With Ink Jet for Source and Drain Electrode of OTFTs," Org. Electron., **11**(5), pp. 854–859.

[23] Jin, H.-J., Park, J., Valluzzi, R., Cebe, P., and Kaplan, D. L., 2004, "Biomaterial Films of Bombyx Mori Silk Fibroin With Poly(Ethylene Oxide)," Biomacromolecules, **5**(3), pp. 711–717.

[24] Viidik, L., Seera, D., Antikainen, O., Kogermann, K., Heinämäki, J., and Laidmäe, I., 2019, "3D-Printability of Aqueous Poly(Ethylene Oxide) Gels," Eur. Polym. J., **120**, p. 109206.

[25] Zheng, D., Bai, B., He, Y., Hu, N., and Wang, H., 2020, "Synthesis and Characterization of Dopamine-Modified Ca-Alginate/Poly(N-Isopropylacrylamide) Microspheres for Water Retention and Multi-Responsive Controlled Release of Agrochemicals," Int. J. Biol. Macromol., **160**, pp. 518–530.

[26] Ouyang, J., 2013, "Secondary Doping' Methods to Significantly Enhance the Conductivity of PEDOT:PSS for Its Application as Transparent Electrode of Optoelectronic Devices," Displays, **34**(5), pp. 423–436.
[27] Mengistie, D. A., Chen, C.-H., Boopathi, K. M., Pranoto, F. W., Li, L.-J., and Chu, C.-W., 2015, "Enhanced Thermoelectric Performance of PEDOT:PSS Flexible Bulky Papers by Treatment With Secondary Dopants," ACS Appl. Mater. Interfaces, **7**(1), pp. 94–100.
[28] Fu, K., Lv, R., Na, B., Zou, S., Zeng, R., Wang, B., and Liu, H., 2019, "Mixed Ion-Electron Conducting PEO/PEDOT: PSS Miscible Blends With Intense Electrochromic Response," Polymer (Guildf.), **184**, p. 121900.
[29] Cao, S., Tong, X., Dai, K., and Xu, Q., 2019, "A Super-Stretchable and Tough Functionalized Boron Nitride/PEDOT:PSS/Poly(N-Isopropylacrylamide) Hydrogel With Self-Healing, Adhesion, Conductive and Photothermal Activity," J. Mater. Chem. A Mater. Energy Sustainable, **7**(14), pp. 8204–8209.
[30] Park, J.-K., Kang, T.-G., Kim, B.-H., Lee, H.-J., Choi, H. H., and Yook, J.-G., 2018, "Real-Time Humidity Sensor Based on Microwave Resonator Coupled With PEDOT:PSS Conducting Polymer Film," Sci. Rep., **8**(1), p. 439.
[31] McDonald, M. B., and Hammond, P. T., 2018, "Efficient Transport Networks in a Dual Electron/Lithium-Conducting Polymeric Composite for Electrochemical Applications," ACS Appl. Mater. Interfaces, **10**(18), pp. 15681–15690.
[32] Zhang, H., Yue, M., Wang, T., Wang, J., Wu, X., and Yang, S., 2021, "Conductive Hydrogel-Based Flexible Strain Sensors With Superior Chemical Stability and Stretchability for Mechanical Sensing in Corrosive Solvents," New J. Chem., **45**(10), pp. 4647–4657.
[33] Jiang, Y., Wang, X., Plog, J., Yarin, A. L., and Pan, Y., 2021, "Electrowetting-Assisted Direct Ink Writing for Low-Viscosity Liquids," J. Manuf. Process., **69**, pp. 173–180.
[34] Plog, J., Jiang, Y., Pan, Y., and Yarin, A. L., 2021, "Electrostatically-Assisted Direct Ink Writing for Additive Manufacturing," Addit. Manuf., **39**, p. 101644.